

# Obtuse isosceles triangles with no stable periodic billiard paths

W. Patrick Hooper

April 11, 2006

Associated to a periodic billiard path  $\hat{\gamma}$  in a triangle  $\Delta$  is the sequence of edges that  $\hat{\gamma}$  hits. We say that  $\hat{\gamma}$  is stable if for any  $\Delta'$  close enough to  $\Delta$ , there is a periodic billiard path  $\hat{\gamma}'$  in  $\Delta'$  that hits the edges of  $\Delta'$  in the same sequence. Earlier, it was demonstrated that right triangles do not admit periodic billiard paths. Now, we intend to show

**Theorem 1** *The obtuse isosceles triangles with angles  $(\pi/2^k, \pi/2^k, \pi - 2\pi/2^k)$  do not admit any stable periodic billiard paths.*

In some sense, this result is quite surprising. Schwartz was able to show that every obtuse triangle with largest angle less than 100 degrees admits a stable periodic billiard path.

As we will describe, the triangles we will be considering “unfold” into Veech surfaces. Veech discovered a geometric property of some special flat surfaces which yields a concrete description of the set of all closed geodesics on the surface [Vee89]. The proof we use of this theorem will make use of these ideas.

In the following section we will find a necessary condition for the stability of a billiard path. We define what it means for a surface to be Veech in the next section, and list some properties of Veech surfaces that will enable us to prove the main result. A combination of these ideas yields an approach to proving that there are no stable periodic billiard paths in a triangles that unfold into a Veech surface.

# 1 Deforming cone surfaces

Let us first define a *cone*. Consider the plane with the origin removed,  $\mathbb{R}^2 \setminus 0$ . Points are identified by their polar coordinates  $(r, \theta)$  with  $r > 0$  and  $\theta$  defined  $(\text{mod } 2\pi)$ . We lift to the universal cover  $\widetilde{\mathbb{R}^2 \setminus 0}$ , where points are identified by  $(r, \theta)$  with  $r > 0$  and  $\theta \in \mathbb{R}$ . The *cone*  $C_\alpha$  with cone angle  $\alpha > 0$  is the surface

$$(\widetilde{\mathbb{R}^2 \setminus 0} / \sim) \cup \{0\}$$

Where  $\sim$  is the equivalence relation on  $\widetilde{\mathbb{R}^2 \setminus 0}$  defined

$$(r_1, \theta_1) \sim (r_2, \theta_2) \text{ if } r_1 = r_2 \text{ and } \theta_1 - \theta_2 \text{ is an integer multiple of } \alpha$$

A *cone surface* is an oriented surface  $S$  with a finite singular set  $\Sigma \subset S$ , so  $S \setminus \Sigma$  is locally isometric to the plane, and each point  $p \in \Sigma$  has a neighborhood  $U_p \subset S$  which is isometric to a subset of a cone  $C_\alpha$  under a map sending  $p$  to the apex of the cone.

A relevant example cone surface  $\mathcal{S}_\Delta$  can be obtained by doubling a triangle  $\Delta$  as in figure 1. Here the cone angles are twice the angles of the triangle.

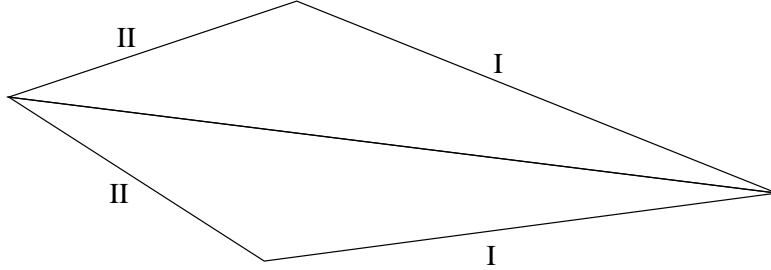


Figure 1: The cone surface  $\mathcal{S}_\Delta$  can be built by doubling a triangle  $\Delta$  across its boundary. The singular set  $\Sigma$  consists of the vertices.

The *billiard flow* on a triangle is the standard geodesic flow on unit tangent vectors based in the interior of the triangle. Tangent vectors on the boundary of the triangle are glued so that the angle of incidence is equal to the angle of reflection. Then the billiard flow “bounces” a vector pointed at an edge of the triangle off the edge, just as you expect the velocity vector of a billiard ball to change when it bounces. In general, the billiard flow can not be well defined at the vertices. A *periodic billiard path* on a triangle is

a loop with speed 1 on the interior of a triangle whose derivative (a loop on the unit tangent space of the triangle with identifications) is invariant under the billiard flow. We do not allow periodic billiard paths to pass through the vertices of the triangle.

The billiard flow on  $\Delta$  can be pulled back under the obvious folding map  $\mathcal{S}_\Delta \rightarrow \Delta$  to the standard geodesic flow on  $\mathcal{S}_\Delta \setminus \Sigma$ . Thus, a periodic billiard path on  $\Delta$  lifts to a loop  $\mathcal{S}_\Delta \setminus \Sigma$ . Conversely a unit speed loop on  $\mathcal{S}_\Delta \setminus \Sigma$  whose derivative is invariant under the geodesic flow can be pushed down to a billiard path on  $\Delta$ .

The primary focus of this paper is on the stability of a billiard path under perturbation of the triangle. It is equivalent to study the stability of geodesics on  $\mathcal{S}_\Delta$  under the perturbation of  $\Delta$ . We notice that the surfaces  $\mathcal{S}_\Delta$  are all naturally homeomorphic, but not isometric. We start with a geodesic  $\gamma$  on  $\mathcal{S}_\Delta \setminus \Sigma$  and extract its homotopy class  $[\gamma]$ . Then we say that  $\gamma$  is *stable* if there is an open neighborhood  $U$  of  $\Delta$  in the space of triangles, so that for any  $\Delta' \in U$  there exists a geodesic  $\gamma' \in [\gamma]$  on  $\mathcal{S}_{\Delta'} \setminus \Sigma$ .

First we will be concerned with deciding when a geodesic  $\gamma$  might be stable on  $\mathcal{S}_\Delta$ . We recall the Gauss-Bonnet theorem applied to surfaces with cone angles which states that if  $S$  is a Riemannian surface with boundary that has Euler characteristic  $\chi(S)$  and cone singularities with cone angles  $\alpha_1 \dots \alpha_n$ , then

$$\int_S K dA = 2\pi\chi(S) - \int_{\partial S} \kappa ds - \sum_{i=1}^n (2\pi - \alpha_i) \quad (1)$$

where  $K dA$  is Gaussian curvature with respect to area and  $\kappa ds$  is the geodesic curvature of the boundary curve with respect to arc length. For our Euclidean cone surfaces,  $K dA \equiv 0$ , therefore

$$\int_{\partial S} \kappa ds = 2\pi\chi(S) - \sum_{i=1}^n (2\pi - \alpha_i) \quad (2)$$

The significance of this integral is that it is invariant under homotopies which avoid the singular set. For  $\partial S$  to be a geodesic,  $\kappa ds$  must be zero.

**Corollary 2 (Application of Gauss-Bonnet)** *If  $\gamma$  is a stable geodesic on  $\mathcal{S}_\Delta \setminus \Sigma$ , then it is null-homologous on  $\mathcal{S}_\Delta \setminus \Sigma$ .*

**Proof:** Enumerate  $\Sigma = \{A, B, C\}$ . The group  $H_1(S_\Delta \setminus \Sigma, \mathbb{Z})$  is isomorphic to  $\mathbb{Z}^2$  and is generated by loops  $\partial A$  and  $\partial B$  which travel once around puncture  $A$  and once around puncture  $B$ .

Notice that the integral  $\int_{\partial S} \kappa ds \pmod{2\pi}$  is a homological invariant of  $S_\Delta \setminus \Sigma$ . By equation 2,

$$\int_{\partial S} \kappa ds \equiv \sum_{i=1}^n \alpha_i \pmod{2\pi}$$

In particular it only depends on the cone angles that the surface  $S$  contains, and not on the topology of  $S$ .

Now consider a geodesic loop  $\gamma$  on  $S_\Delta \setminus \{A, B, C\}$ . We write the homology class  $[\gamma] = a[\partial A] + b[\partial B]$ . In other words, the loop  $\gamma$  is homologically equivalent to  $a$  disks containing  $A$  and  $b$  disks containing  $B$ . Then

$$\int_{\gamma} \kappa ds \equiv a\alpha_A + b\alpha_B \pmod{2\pi}$$

where  $\alpha_A$  and  $\alpha_B$  are the cone angles at  $A$  and  $B$ . As we vary the triangle,  $\alpha_A$  and  $\alpha_B$  vary independently (they are just twice two of the angles of the triangle). Therefore,  $\int_{\gamma} \kappa ds$  can be identically zero on an open set only if  $a = b = 0$ , so that  $\gamma$  is null-homologous.  $\diamond$

**Remark 3** *In fact, the converse of 2 is true as well. That is, if  $\gamma$  is a geodesic on  $S_\Delta \setminus \Sigma$ , then  $\gamma$  is null-homologous implies that  $\gamma$  is stable. To verify this fact, we would verify that the existence of a geodesic in a null-homologous homotopy class of  $S_\Delta$  depends only on an open condition in the angles of the triangle  $\Delta$ .*

## 2 Veech surfaces

A *translation surface* is a topological surface  $S$  together with a singular set  $\Sigma$  and an atlas of charts from  $S \setminus \Sigma$  to the plane so that the transition functions are translations. The *singular set* is just a discrete set of points. The *atlas of charts* is a covering of  $S \setminus \Sigma$  by open sets  $U_i$  together with local homeomorphisms  $\phi_i : U_i \rightarrow \mathbb{R}^2$ . The *transition functions* are the maps  $\phi_i \circ \phi_j^{-1}$  restricted to  $\phi_j(U_i \cap U_j)$ . The translation surface inherits the pull

back metric from the plane and also the notion of direction. The structure at the singular set  $\Sigma$  can be interpreted as a Euclidean cone structure with an angle that is an integer multiple of  $2\pi$ . We will primarily be concerned with the translation surfaces depicted in figure 2. A thorough discussion of these translation surfaces appears in the next section.

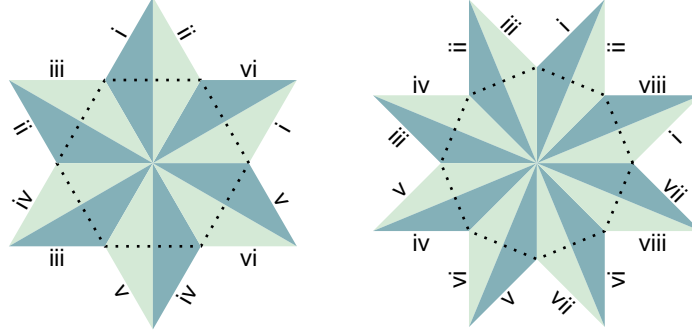


Figure 2: Translation surfaces built out of the triangles  $\Delta_{2m}$  with angles  $(\frac{\pi}{2m}, \frac{\pi}{2m}, \frac{(m-1)\pi}{m})$ , for  $m = 3, 4$ . Notice that the same surface can be built out of two regular  $2m$ -gons, glued so that each edge of the first is glued to the opposite side of the second.

Let  $\widehat{SL}(2, \mathbb{R})$  be the subgroup of the affine group of the plane which fixes the origin and preserves unsigned area. That is,  $\widehat{SL}(2, \mathbb{R})$  is the Lie group

$$\widehat{SL}(2, \mathbb{R}) = \{M \in GL(2, \mathbb{R}) | \text{Det}(M) = \pm 1\} \quad (3)$$

This matrix group just acts linearly on points in  $\mathbb{R}^2$  in the usual way.

There is an action of  $\widehat{SL}(2, \mathbb{R})$  on translation surfaces. If  $A \in \widehat{SL}(2, \mathbb{R})$  and  $S$  is a translation surface, then we build a new translation surface  $A(S)$  by post-composing each chart map  $\phi_i : U_i \rightarrow \mathbb{R}^2$  with  $A$ . The *Veech group* of a translation surface  $S$  is the subgroup  $\Gamma(S) \subset \widehat{SL}(2, \mathbb{R})$  consisting of those  $A \in \widehat{SL}(2, \mathbb{R})$  for which there is an isometry  $f_A : S \rightarrow A(S)$  which preserves directions. The condition that it preserves directions is essential, since otherwise any rotation would be in the Veech group. Since the surfaces  $S$  and  $A(S)$  are canonically homeomorphic under the action of  $A$ , the elements  $\{f_A | A \in \Gamma(S)\}$  are homeomorphisms from the surface to itself. We therefore consider  $f_A$  to be an element of the mapping class group of the surface. These elements also permute the points in the singular set and preserve cone angles.

We denote the mapping class group of the surface  $S$  fixing the singular set  $\Sigma$  by  $\mathcal{MCG}(S, \Sigma)$  and use  $V(S)$  to denote this particular subgroup.

A parabolic in  $\widehat{SL}(2, \mathbb{R})$  is an element which fixes a single direction  $\theta$  in  $\mathbb{R}^2$ , so it has a single eigenvector. Veech showed that having a parabolic in the Veech group has implications for the dynamics of the geodesic flow in the direction  $\theta$ , namely all but finitely many geodesics traveling in the direction  $\theta$  close up. A *saddle connection* is a geodesic segment which starts at a point on  $\Sigma$  and ends at a point on  $\Sigma$  but hits no elements of  $\Sigma$  on its interior.

**Lemma 4 (Veech)** *If  $A \in \Gamma(S)$  is a parabolic preserving the direction  $\theta$ , then there is a decomposition of the surface into cylinders by cutting along saddle connections in the direction of  $\theta$ . The corresponding homeomorphism  $f_A$  acts as a Dehn twist in each of the cylinders.*

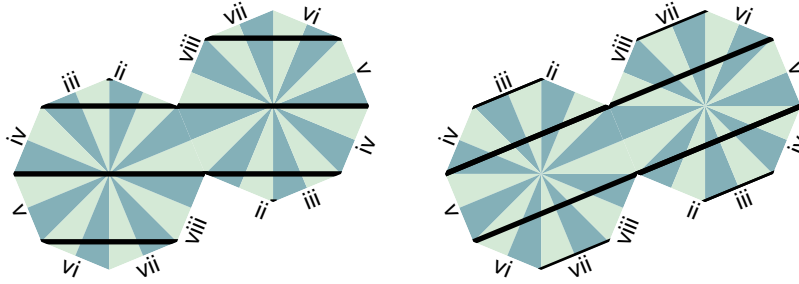


Figure 3: There is a parabolic which preserves each of these decompositions of a translation surface into cylinders.

Given a decomposition of a translation surface into parallel cylinders, a necessary and sufficient condition for there to be a parabolic automorphism fixing the direction of the decomposition is that the ratios of the lengths to the widths of the cylinders must be commensurable (differ by multiplication by a rational number). For example, consider the decompositions of the translation surface depicted in figure 3.

Assuming the radius of the octagons depicted in figure 3 is 1, the lengths and widths of each cylinder shown can be expressed in the form

$$l = 2 \left( \cos \left( \frac{\pi}{8}(k+1) \right) + \cos \left( \frac{\pi}{8}(k-1) \right) \right)$$

$$w = \sin \left( \frac{\pi}{8}(k+1) \right) - \sin \left( \frac{\pi}{8}(k-1) \right)$$

for some integer  $k$ . The angle addition formulas can then be used to show that for each  $k$

$$\frac{l}{m} = \frac{2 \cos(\frac{\pi}{8})}{\sin(\frac{\pi}{8})}$$

Since this value is independent of  $k$ , it follows that there are parabolic automorphisms of this surface which fix the directions of the cylinder decompositions. This example is a double cover of one of Veech's original examples. See [Vee89].

Veech showed that if the Veech group  $\Gamma(S)$  is a lattice then the dynamics of the billiard flow satisfy a dichotomy. See [MT02] or [Vee89].

**Theorem 5 (Veech dichotomy)** *Suppose  $\Gamma(S)$  is a lattice. It can not be co-compact. In every direction  $\theta$  on the surface  $S$  the foliation of geodesics traveling in direction  $\theta$  is either*

1. *completely periodic. That is, all leaves are closed or saddle connections.*
2. *minimal. Here, every leaf is dense.*

*Furthermore, if the direction  $\theta$  is completely periodic, then there is a parabolic in  $\Gamma(S)$  which fixes the direction  $\theta$ .*

We can use these results to list off all the homotopy classes of  $S \setminus \Sigma$  containing geodesics.

**Corollary 6** *Suppose  $S$  is a translation surface and  $\Gamma(S)$  is a lattice. There is a finite list of homotopy classes of curves containing geodesics  $[\gamma_1], \dots, [\gamma_s]$  so that for every homotopy class  $[\eta]$  containing a geodesic, there is an element of the Veech group  $f_A \in V(S)$  so that  $[\eta] = f_A([\gamma_i])$  for some  $i$ .*

**Proof:**  $\widehat{SL}(2, \mathbb{R})/\pm 1$  acts as the isometry group of the hyperbolic plane  $\mathbb{H}^2$ . We look at the orbifold  $X(S) = \mathbb{H}^2/\Gamma^+(S)$ , where  $\Gamma^+(S)$  is the orientation preserving subgroup of  $\Gamma(S)$ . (The surface  $X(S)$  may have orbifold points coming from finite order elliptics in  $\Gamma(S)$ .) The orbifold  $X(S)$  is known as the Teichmüller curve.  $X(S)$  is a finite volume hyperbolic orbifold which must contain punctures, which we list off as  $p_1, \dots, p_s$ . Each puncture  $p_i$  gives rise to a conjugacy class  $[P_i]$  of parabolics in  $\Gamma(S)$ , realizing the holonomy of a loop traveling around  $p_i$ . We make an arbitrary choice of a parabolic  $P_i \in [P_i]$  for each  $i$ . Veech's dichotomy tells us that in the direction fixed by

$P_i$ , there is a decomposition into cylinders  $C_{i,j}$ . For each cylinder, we get a homotopy class  $[\gamma_{i,j}]$  containing a geodesic. Because every parabolic in the Veech group is conjugate to some  $P_i$ , every homotopy class of  $S$  containing a geodesic is the image of one of the homotopy classes  $[\gamma_{i,j}]$  under an element of the Veech group  $V(S) \subset \mathcal{MCG}(S, \Sigma)$ . Indeed, since  $V(S)$  is finitely generated, we can express the set of all closed geodesics on  $S$  with a finite amount of information.  $\diamond$

### 3 The $(\frac{\pi}{2m}, \frac{\pi}{2m}, \frac{\pi(m-1)}{m})$ triangles

Given a triangle  $\Delta$  with edges marked 1,2,3, we can build a translation surface by “unfolding” the triangle. Consider the action of the group  $\mathbb{Z}_2 * \mathbb{Z}_2 * \mathbb{Z}_2$  generated by reflections in the sides of the triangle. Take all images of  $\Delta$  under this group action. We identify any two triangles which differ by a translation, and glue two edges together if the triangles differ by a reflection in that edge. The result is a translation surface, which we call the minimal translation surface associated to  $\Delta$ . This surface is denoted  $MT_\Delta$ . There is a natural folding map from  $MT_\Delta \rightarrow \Delta$ . We will say the singular set of  $MT_\Delta$  is the subset  $\Sigma \subset MT_\Delta$  which is mapped to the vertices of the triangle.

We are interested in the triangles  $\Delta_{2m}$  with angles  $(\frac{\pi}{2m}, \frac{\pi}{2m}, \frac{\pi(m-1)}{m})$ . To simplify notation, denote the surface associated minimal translation surfaces  $MT_{\Delta_{2m}}$  by  $MT_{2m}$ . These surfaces can also be constructed by taking two regular  $2m$ -gons and gluing each edge of the first polygon to the opposite edge of the second polygon. See figure 2. The surfaces  $MT_{2m}$  are double covers of Veech’s original examples of a regular  $2m$ -gon with opposite edges identified (see [Vee89]).

Recall,  $\mathcal{S}_{\Delta_{2m}}$  was the Euclidean cone surface which is the double of the triangle  $\Delta_{2m}$  along its boundary. We denote  $\mathcal{S}_{\Delta_{2m}}$  by  $\mathcal{S}_{2m}$ . The singular set of  $\mathcal{S}_{2m}$  is the collection of cone points,  $\Sigma$ . The surface  $MT_{2m}$  is a branched cover of  $\mathcal{S}_{2m}$  over the singular set  $\Sigma$ .

Each translation surface  $MT_{2m}$  is a Veech surface. In order to use corollary 6 to list homotopy classes containing geodesics, we will need to understand the groups  $\Gamma(MT_{2m}) \subset \widehat{SL}(2, \mathbb{R})$  and  $V(MT_{2m}) \subset \mathcal{MCG}(S, \Sigma)$ . These groups are closely related to triangle groups. We define the  $(\infty, \infty, \infty)$  triangle group,  $\mathcal{T}_\infty$ , to be the free product  $\mathbb{Z}_2 * \mathbb{Z}_2 * \mathbb{Z}_2$ . Each  $\mathbb{Z}_2$  factor is reflection one of the sides of a triangle. We specify generators for  $\mathcal{T}_\infty$  in an alternate



way:

$$\mathcal{T}_\infty = \langle i, j, D \mid i^2 = j^2 = (iD)^2 = 1 \rangle \quad (4)$$

The  $(m, \infty, \infty)$  triangle group,  $\mathcal{T}_m$ , is the  $\mathcal{T}_\infty$  triangle modulo the additional relation,  $(i \circ j)^m = 1$ .

**Proposition 7 (The groups  $V(\mathbf{MT}_{2m})$ )** *The Veech group  $V(MT_{2m})$  is isomorphic to the direct product  $\mathcal{T}_{2m} \times \mathbb{Z}_2$ . Take generators for  $\mathcal{T}_{2m}$  as in equation 4 and use  $h$  to denote the generator of  $\mathbb{Z}_2$ . Let  $\rho_{2m} : \mathcal{T}_{2m} \times \mathbb{Z}_2 \rightarrow V(MT_{2m})$  be this isomorphism. The generators act as follows*

1. *The action of  $\rho_{2m}(h)$  is automorphism of the cover mapping  $MT_{2m}$  to Veech's original surface obtained by gluing opposite sides of the regular  $2m$ -gon together by translations. In other words, the generator of the  $\mathbb{Z}_2$  swaps the decomposition into two regular  $2m$ -gons shown in figures 4-6, preserving directions in the translation surface.*
2. *The action of  $\rho_{2m}(i)$  is by Euclidean reflection in the horizontal lines shown in figure 4.*
3. *The action of  $\rho_{2m}(j)$  is by Euclidean reflection in the nearly horizontal lines show in figure 5.*
4. *The action of  $\rho_{2m}(D)$  is by Dehn twists in the vertical cylinder decomposition. See figure 6.*

There is a surjective group homomorphism  $V(MT_{2m}) \rightarrow \Gamma(MT_{2m}) \subset \widehat{SL}(2, \mathbb{R})$ . The kernel of this homomorphism consists of elements of  $V(MT_{2m})$  which preserve directions on  $MT_{2m}$ . This is exactly the  $\mathbb{Z}_2$  factor, since only  $\rho_{2m}(h)$  preserves directions on  $MT_{2m}$ .

**Proposition 8 (The Veech groups  $\Gamma(\mathbf{MT}_{2m})$ )** *The Teichmüller curve,  $X(MT_{2m}) = \mathbb{H}^2 / \Gamma^+(MT_{2m})$ , is a doubled hyperbolic triangle with two ideal vertices and one vertex with angle  $\frac{\pi}{m}$ . By corollary 6, up to the action of the Veech group, there are exactly two decompositions into parallel cylinders. We can choose the vertical and the slightly off-vertical direction. Figure 7 shows one curve in the center of every such cylinder.*

Let us now describe a minimal list of ingredients necessary to prove that  $\Delta_{2m}$  has no stable periodic billiard paths, for  $m$  a power of two.

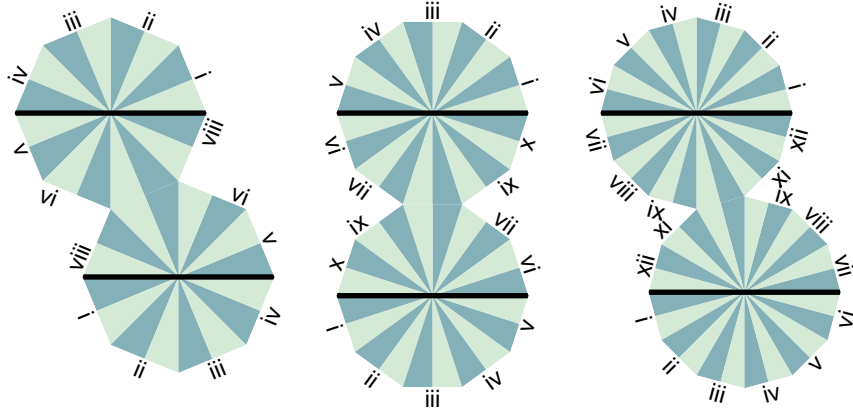


Figure 4: The generator  $\rho_{2m}(i)$  acts by Euclidean reflection in these vertical lines.

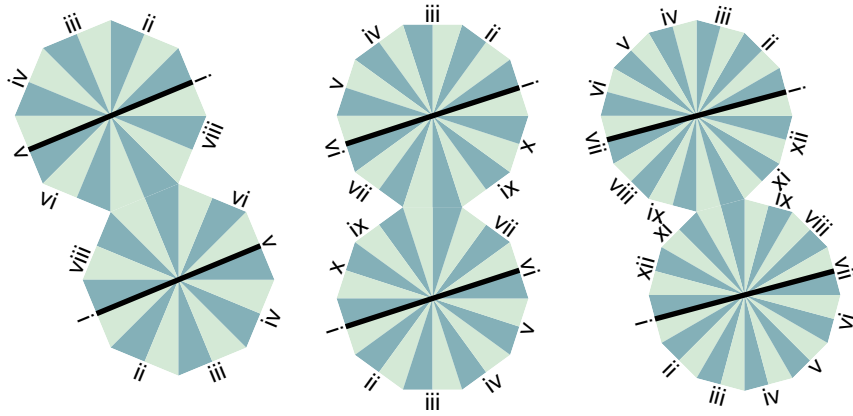


Figure 5: The generator  $\rho_{2m}(j)$  acts by Euclidean reflection in these slightly off vertical lines.

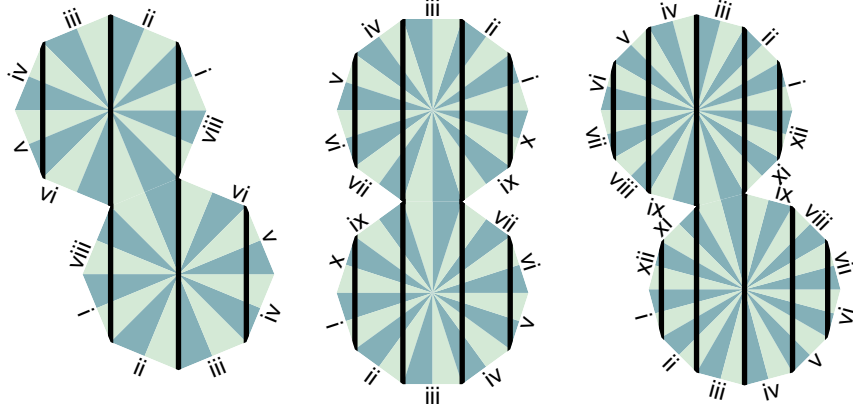


Figure 6: The generator  $\rho_{2m}(D)$  acts by a Dehn twist in this vertical cylinder decomposition. All the cylinders depicted have the same moduli, so  $D$  acts by a single Dehn twist in each cylinder.

1. The minimal translation surface  $MT_{2m}$  with singular set  $\Sigma$ .
2. The group  $V(MT_{2m})$  acting on the first homology group  $H_1(MT_{2m} \setminus \Sigma, \mathbb{Z})$ .
3. A finite collection of homology classes  $F_{2m} = \{\llbracket \gamma_1 \rrbracket, \dots, \llbracket \gamma_{2m} \rrbracket\}$  (shown in figure 7). Under the action of  $V(MT_{2m})$ , this finite collection of curves hits every homology class which contains a geodesic by corollary 6.
4. The covering  $\phi_{2m} : MT_{2m} \rightarrow \mathcal{S}_{2m}$ .

Under these circumstances we know by corollaries 2 and 6, that

**Corollary 9** *If there is a stable periodic billiard path in  $\Delta_{2m}$ , then there is a homology class  $\llbracket \gamma_i \rrbracket \in F_{2m}$  and an element  $f \in V(MT_{2m})$  so that*

$$\phi_{2m} \circ f(\llbracket \gamma_i \rrbracket) = 0 \in H_1(\mathcal{S}_{2m} \setminus \Sigma, \mathbb{Z})$$

We will use this idea to demonstrate the result that for  $m$  a power of two,  $\Delta_{2m}$  has no stable periodic billiard paths. We break our argument into two cases. The first and easier case deals with the special pair of curves in  $F_{2m}$  which bound an annulus. See figure 8. In the second case we deal with the remaining curves.

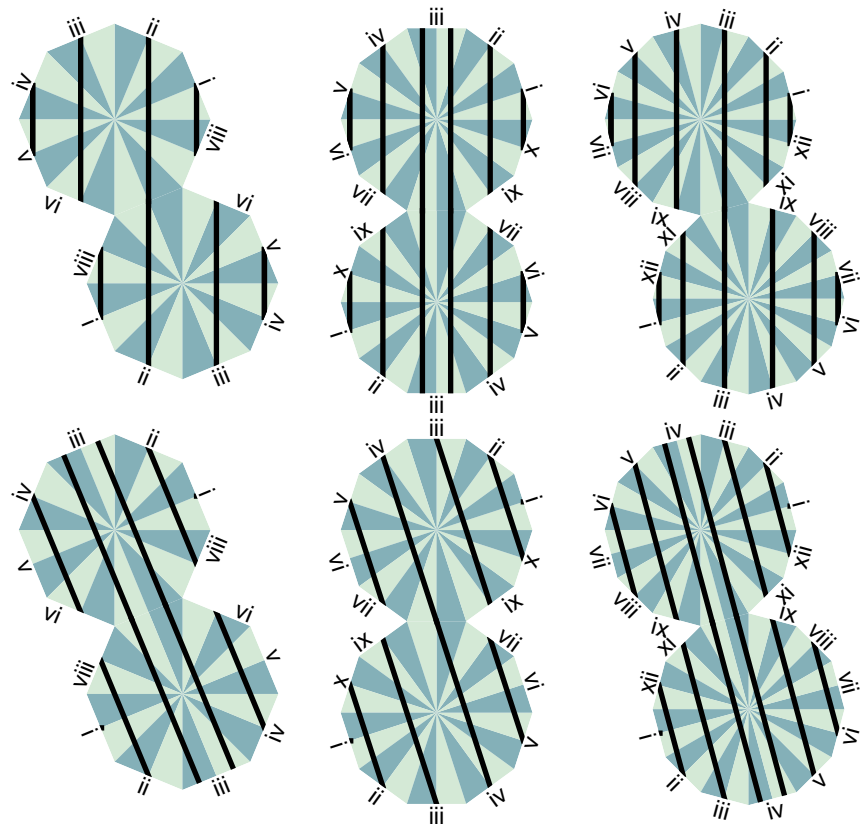


Figure 7: Every homotopy class containing a geodesic in  $MT_{2m}$  is the image of a homotopy class of curves in one of these two decompositions under  $V(MT_{2m})$ .

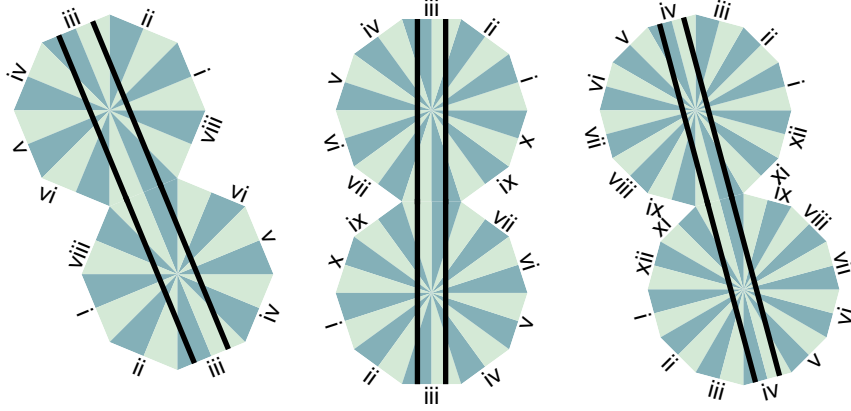


Figure 8: These pairs of curves bound an annulus in  $MT_{2m}$ .

## 4 Curves that bound an annulus

As in the right side of figure 9, we use  $A$ ,  $B$ , and  $C$  to denote the cone points of  $\mathcal{S}_{2m}$ . We use  $\partial A$  and  $\partial B$  to denote curves in  $\mathcal{S}_{2m} \setminus \Sigma$  which travel around  $A$  and  $B$  respectively in the counter-clockwise direction. Then  $[\partial A]$  and  $[\partial B]$  generate  $H_1(\mathcal{S}_{2m} \setminus \Sigma, \mathbb{Z}) \cong \mathbb{Z}^2$ .

**Proposition 10** *If  $[\gamma] \in H_1(\mathcal{S}_{2m} \setminus \Sigma, \mathbb{Z})$  is one of the homology classes of curves coming from figure 8 then for all  $f \in V(MT_{2m})$*

$$\phi_{2m} \circ f([\gamma]) = \pm m([\partial A] + [\partial B]) \neq 0 \in H_1(\mathcal{S}_{2m} \setminus \Sigma, \mathbb{Z})$$

**Proof:** Call the two curves of figure 8  $\gamma_1$  and  $\gamma_2$  and the annulus they bound  $\mathcal{A}$ . We orient the curves in opposite directions, so that  $\partial \mathcal{A} = \gamma_1 \cup \gamma_2$  is the oriented boundary of the annulus the curves enclose. We label the points in the singular set of  $MT_{2m}$  by their images under the map  $\phi_{2m} : MT_{2m} \rightarrow \mathcal{S}_{2m}$ . See figure 9.

Note that the Euclidean isometry of  $MT_{2m}$  which acts as a rotation by  $\pi$  preserving the points  $A$  and  $B$  of figure 9. This isometry is an automorphism of the cover  $\phi_{2m} : MT_{2m} \rightarrow \mathcal{S}_{2m}$ . Therefore,

$$\phi_{2m}([\gamma_1]) = \phi_{2m}([\gamma_2]) \tag{5}$$

On  $MT_{2m}$ , the pair of curves  $\gamma_1 \cup \gamma_2$  is homologically the same as a pair of loops, one of which travels around  $A$  once and the other which travels around

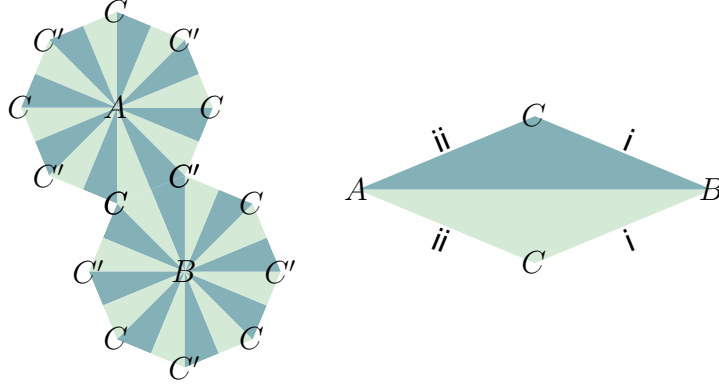


Figure 9: The points in the singular set of  $MT_{2m}$  labeled the same as their images in  $\mathcal{S}_{2m}$ . There is only one preimage of  $A$  and  $B$ , but there are two pre-images of  $C$ .

$B$  once. Therefore, the homology class  $\phi_{2m}(\llbracket \gamma_1 \rrbracket + \llbracket \gamma_2 \rrbracket)$  wraps  $2m$  times around the vertex  $A$  on  $\mathcal{S}_{2m}$  and  $2m$  times around the vertex  $B$ . Therefore,  $\phi_{2m}(\llbracket \gamma_1 \rrbracket + \llbracket \gamma_2 \rrbracket)$  is not null homologous. By equation 5, it must be that  $\phi_{2m}(\llbracket \gamma_1 \rrbracket)$  wraps  $m$  times around both  $A$  and  $B$  therefore,

$$\phi_{2m}(\llbracket \gamma_1 \rrbracket) = m(\llbracket \partial A \rrbracket + \llbracket \partial B \rrbracket)$$

We can extend this argument to the curves  $f(\gamma_1)$  and  $f(\gamma_2)$  for all  $f \in V(MT_{2m})$  if we can show  $A, B \in f(\mathcal{A})$ . This follows from the fact that the pair of points  $A, B \subset MT_{2m}$  is fixed by the action of  $V(MT_{2m})$ , which is generated by  $\rho_{2m}(h)$ ,  $\rho_{2m}(i)$ ,  $\rho_{2m}(j)$ , and  $\rho_{2m}(D)$ . Recall proposition 7. From the description of these actions, it is easy to verify

1.  $\rho_{2m}(h)$  swaps  $A$  with  $B$  and preserves orientation.
2.  $\rho_{2m}(i)$  and  $\rho_{2m}(j)$  preserve both  $A$  and  $B$ , but reverse orientation.
3. If  $m$  is even,  $\rho_{2m}(D)$  preserves  $A$  and  $B$ , and preserves orientation. In this case,  $A$  and  $B$  lie on the boundaries of the cylinders where Dehn twists are being performed. All points on the boundary of a cylinder where a Dehn twist is being preserved are fixed.
4. If  $m$  is odd,  $\rho_{2m}(D)$  swaps  $A$  with  $B$ , and preserves orientation. Here,  $A$  and  $B$  lie in the center of a cylinder and are equally spaced apart.

In the center of a cylinder, an affine Dehn twist moves points half way around the cylinder.

Therefore, for all  $f \in V(MT_{2m})$ , we know that

$$\phi_{2m} \circ f(\llbracket \gamma_1 \rrbracket) = \begin{cases} m(\llbracket \partial A \rrbracket + \llbracket \partial B \rrbracket) & \text{if } f \text{ preserves orientation} \\ -m(\llbracket \partial A \rrbracket + \llbracket \partial B \rrbracket) & \text{if } f \text{ reverses orientation} \end{cases}$$

◇

## 5 The remaining curves

In this section we deal with curves that appear in figure 7, but not in figure 8. The central idea is to reduce via topological covering maps to the argument used in the previous section.

The singular set  $\Sigma$  associated to the surface  $MT_{2m}$ , has a pair removable singularities. The cone angles at the points  $A$  and  $B$  of figure 9 are  $2\pi$ . Therefore, we can remove them from the singular set. We define the reduced singular set  $\Sigma' = \Sigma \setminus \{A, B\}$ .

Unfortunately, there is a cost for removing these removable singularities. Namely, the curves which travel once around  $A$  or  $B$  in  $MT_{2m}$  are null homologous in  $MT_{2m} \setminus \Sigma'$ , but not in  $MT_{2m} \setminus \Sigma$ . The homology classes of these curves are sent by  $\phi_{2m} : MT_{2m} \setminus \Sigma \rightarrow \mathcal{S}_{2m}$  to  $2m\llbracket \partial A \rrbracket$  and  $2m\llbracket \partial B \rrbracket$  respectively. Therefore, we can only define the induced map on homology modulo  $2m$ . The induced map on homology gives the map:

$$\phi_{2m} : H_1(MT_{2m} \setminus \Sigma', \mathbb{Z}) \rightarrow H_1(\mathcal{S}_{2m}, \mathbb{Z}_{2m}) \quad (6)$$

The advantage of removing these singularities comes from a covering relationship between the objects involved. For any positive integer  $k$ , we can view the topological surface  $MT_{2km}$  as a  $k$ -fold branched cover of  $MT_{2m}$  branched over the points of  $\Sigma$ . Given  $MT_{2km}$ , the topological surface  $MT_{2m}$  can be obtained as  $MT_{2km}$  modulo the action of  $(i \circ j)^{2m}$ , which acts as a Euclidean rotation by  $\frac{2\pi}{k}$  and preserves the decomposition of  $MT_{2km}$  into regular  $2km$ -gons. Denote this covering map by  $\psi_k : MT_{2km} \rightarrow MT_{2m}$ . See figure 10.

To carefully define this covering map, we number the triangles of  $MT_{2km}$  from 0 to  $4km - 1$ . We assign the numbers so that they increase as we travel

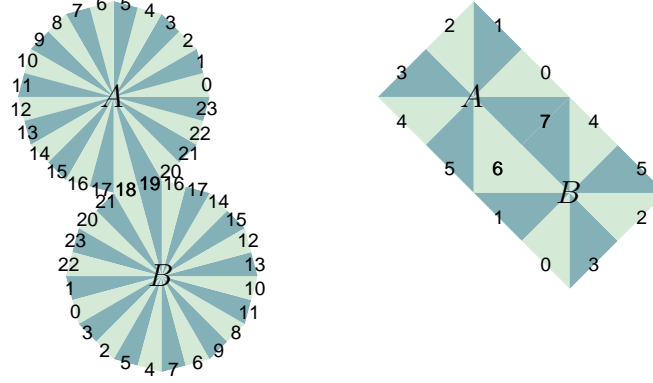


Figure 10: The cover  $\psi_3 : MT_{12} \rightarrow MT_4$  sends triangles marked  $x$  to triangles marked  $x \pmod{8}$ .

in the counter-clockwise direction around  $A$ . We mark the triangles of  $MT_{2m}$  in the same manner from 0 to  $4m - 1$ . Then we define the covering map  $\psi_k$  to be the map which preserves the labels at the points  $A$  and  $B$  and sends each triangle labeled  $t$  to the triangle labeled  $t \pmod{4m}$ .

We need to understand how these covering maps act on the objects we care about. Consider the collection of objects:

1. The surface  $MT_{2m}$  with singular set  $\Sigma'$ .
2. The group action  $\rho_{2m} : \mathcal{T}_\infty \times \mathbb{Z}_2 \rightarrow \text{Aut}(H_1(MT_{2m} \setminus \Sigma', \mathbb{Z}))$  generated by the actions  $\rho_{2m}(h)$ ,  $\rho_{2m}(i)$ ,  $\rho_{2m}(j)$ , and  $\rho_{2m}(D)$ .
3. The finite collection of homology classes  $F'_{2m}$  of curves appearing in figure 7, but not in figure 8.
4. The map on homology induced by the covering  $MT_{2m} \rightarrow \mathcal{S}_{2m}$ :

$$\phi_{2m} : H_1(MT_{2m} \setminus \Sigma', \mathbb{Z}) \rightarrow H_1(\mathcal{S}_{2m} \setminus \Sigma, \mathbb{Z}_{2m})$$

**Remark 11** *In order to avoid inundating our argument with needless special cases, we note the objects we are considering are not geometric, but are topological. We defined the surfaces  $MT_{2m}$  for  $m \geq 3$ . We can also consider the translation surface  $MT_4$  associated to the triangle  $\Delta_4$  with angles  $(\frac{\pi}{4}, \frac{\pi}{4}, \frac{\pi}{2})$ . We can define the surface  $MT_2$  associated to the triangle  $\Delta_2$*



with angles  $(\frac{\pi}{2}, \frac{\pi}{2}, 0)$ .  $\Delta_2$  is a degenerate triangle, which we can envision as an infinitely long rectangular strip (i.e.  $\mathbb{R}_{\geq 0} \times [0, 1]$ ). For  $MT_4$  everything we have discussed still makes sense.  $MT_2$  is a standard infinite Euclidean cylinder with two punctures ( $A$  and  $B$ ). Everything makes sense here except possibly the action of  $\rho_2(D)$ , which acts on homology as a Dehn twist in this cylinder. Even proposition 10 makes sense for these surfaces.

The covering map  $\psi_k$  behaves nicely with respect to the collection of objects above.

**Lemma 12** *The covering map  $\psi_k$  satisfies the following*

1.  $\psi_k$  sends the singular set  $\Sigma' \subset MT_{2km}$  to  $\Sigma' \subset MT_{2m}$ .
2. For all elements  $x \in \mathcal{T}_\infty \times \mathbb{Z}_2$ , there is an  $x' \in \mathcal{T}_\infty \times \mathbb{Z}_2$  so that the following diagram commutes:

$$\begin{array}{ccc} H_1(MT_{2km} \setminus \Sigma', \mathbb{Z}) & \xrightarrow{\rho_{2km}(x)} & H_1(MT_{2km} \setminus \Sigma', \mathbb{Z}) \\ \psi_k \downarrow & & \psi_k \downarrow \\ H_1(MT_{2m} \setminus \Sigma', \mathbb{Z}) & \xrightarrow{\rho_{2m}(x')} & H_1(MT_{2m} \setminus \Sigma', \mathbb{Z}) \end{array} \quad (7)$$

3. We use the identity map  $id : (\mathcal{S}_{2km}, \Sigma) \rightarrow (\mathcal{S}_{2m}, \Sigma)$  to identify the two spheres and the labeled cone points. The following diagram commutes

$$\begin{array}{ccc} H_1(MT_{2km} \setminus \Sigma', \mathbb{Z}) & \xrightarrow{\phi_{2km}} & H_1(\mathcal{S}_{2km} \setminus \Sigma, \mathbb{Z}_{2km}) \\ \psi_k \downarrow & & id \downarrow \\ H_1(MT_{2m} \setminus \Sigma', \mathbb{Z}) & \xrightarrow{\phi_{2m}} & H_1(\mathcal{S}_{2m} \setminus \Sigma, \mathbb{Z}_{2m}) \end{array} \quad (8)$$

**Proof:** Item 1 is trivial. Item 3 follows from the fact that  $MT_{2m}$  is an intermediate branched covering of  $MT_{2km} \rightarrow \mathcal{S}_{2km} = \mathcal{S}_{2m}$ .

Item 2 is much more difficult, and slightly tedious. We postpone the proof of this fact until the next section.  $\diamond$

The point of this lemma, is the following

**Corollary 13** Suppose  $\gamma$  is a curve on  $MT_{2km}$  and  $\eta = \psi_k(\gamma)$  is its image in  $MT_{2m}$ . If for all  $x \in \mathcal{T}_\infty \times \mathbb{Z}_2$ ,

$$\phi_{2m} \circ \rho_{2m}(x)(\llbracket \eta \rrbracket) \neq 0 \in H_1(\mathcal{S}_{2m} \setminus \Sigma, \mathbb{Z}_{2m}) \quad (9)$$

then for all  $x \in \mathcal{T}_\infty \times \mathbb{Z}_2$ ,

$$\phi_{2km} \circ \rho_{2km}(x)(\llbracket \gamma \rrbracket) \neq 0 \in H_1(\mathcal{S}_{2km} \setminus \Sigma, \mathbb{Z}_{2km}) \quad (10)$$

**Proof:** Assume statement 9. By the lemma, for all  $x \in \mathcal{T}_\infty \times \mathbb{Z}_2$ , there is an  $x' \in \mathcal{T}_\infty \times \mathbb{Z}_2$  so that the following diagram commutes:

$$\begin{array}{ccccc} H_1(MT_{2km} \setminus \Sigma', \mathbb{Z}) & \xrightarrow{\rho_{2km}(x)} & H_1(MT_{2km} \setminus \Sigma', \mathbb{Z}) & \xrightarrow{\phi_{2km}} & H_1(\mathcal{S}_{2km} \setminus \Sigma, \mathbb{Z}_{2km}) \\ \psi_k \downarrow & & \psi_k \downarrow & & id \downarrow \\ H_1(MT_{2m} \setminus \Sigma', \mathbb{Z}) & \xrightarrow{\rho_{2m}(x')} & H_1(MT_{2m} \setminus \Sigma', \mathbb{Z}) & \xrightarrow{\phi_{2m}} & H_1(\mathcal{S}_{2m} \setminus \Sigma, \mathbb{Z}_{2m}) \end{array} \quad (11)$$

Since  $\phi_{2m} \circ \rho_{2m}(x')(\llbracket \eta \rrbracket) \neq 0 \in H_1(\mathcal{S}_{2m} \setminus \Sigma, \mathbb{Z}_{2m})$  for all  $x'$ , statement 10 must hold as well.  $\diamond$

Now we can prove theorem 1. Recall, the theorem stated that the triangles with angles  $(\pi/2^k, \pi/2^k, \pi - 2\pi/2^k)$  do not have any stable periodic billiard paths.

**Proof of Theorem 1:** Assume  $m$  is a power of two. Let  $2^k = 2m$ . By corollary 9, it is sufficient to show that if  $\gamma$  is a curve which shows up in figure 7, then for all elements  $x \in \mathcal{T}_\infty \times \mathbb{Z}_2$ ,

$$\phi_{2^k} \circ \rho_{2^k}(x)(\llbracket \gamma \rrbracket) \neq 0 \in H_1(\mathcal{S}_{2^k} \setminus \Sigma, \mathbb{Z}) \quad (12)$$

Proposition 10 proved this statement for the special case of the curves appearing in figure 8.

The remaining curves are depicted in figure 11. We organize this list by numbering the midpoint in the long side of the each isosceles triangle in  $MT_{2^k}$ . We use elements of  $\mathbb{Z}_{2^k}$  and number counter-clockwise around the top  $2^k$ -gon. Our curves are labeled  $\gamma(a, b)$  for  $a, b \in \mathbb{Z}_{2^k}$ . Note that the difference  $a - b \pmod{2^k}$  is never equal to 0 or  $2^{k-1}$ . Then we can find an  $1 \leq j < k$  so that

$$a - b \equiv 2^{j-1} \pmod{2^j}$$

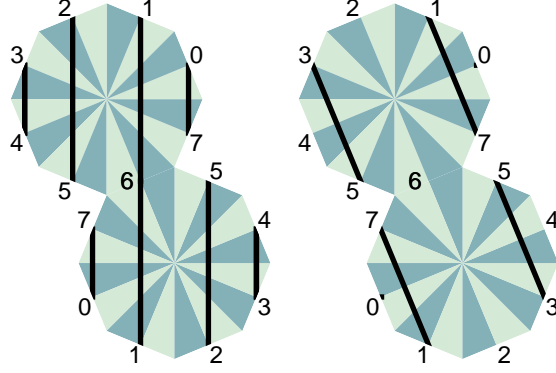


Figure 11: The remaining curves dealt with in the proof of Theorem 1 for  $m = 4$ .

(Choose  $j - 1$  to be the biggest power of two dividing  $a - b$ .)

Consider the branched cover  $\psi_{2^{k-j}} : MT_{2^k} \rightarrow MT_{2^j}$ . The image  $\eta = \psi_{2^{k-j}}(\gamma(a, b))$  is a curve which travels from a midpoint marked  $a \pmod{2^j}$  to a midpoint marked  $a + 2^{j-1} \pmod{2^j}$ . After a rotation (of the form  $\rho_{2^j}((i \circ j)^n)$  for some  $n$ ) we can see  $\eta$  is homologically equivalent to one of the special curves of figure 8. Then by proposition 10, for all  $x \in \mathcal{T}_\infty \times \mathbb{Z}_2$ ,

$$\phi_{2^j} \circ \rho_{2^j}(x)(\llbracket \eta \rrbracket) = 2^{j-1}(\llbracket \partial A \rrbracket + \llbracket \partial B \rrbracket) \neq 0 \in H_1(\mathcal{S}_{2m} \setminus \Sigma, \mathbb{Z}_{2^j})$$

Finally by corollary 13, it follows that for all  $x \in \mathcal{T}_\infty \times \mathbb{Z}_2$ ,

$$\phi_{2^k} \circ \rho_{2^k}(x)(\llbracket \gamma \rrbracket) \neq 0 \in H_1(\mathcal{S}_{2m} \setminus \Sigma, \mathbb{Z}_{2^k})$$

and therefore  $\phi_{2^k} \circ \rho_{2^k}(x)(\llbracket \gamma \rrbracket)$  is not equal to zero in  $H_1(\mathcal{S}_{2m} \setminus \Sigma, \mathbb{Z})$  either.  $\diamond$

## 6 Proof of Lemma 12, item 2

**Proof of Lemma 12, item 2:** We prove the statement on the generators  $h$ ,  $i$ ,  $j$ , and  $D$ .

1. The action of  $\rho_{2km}(i)$  on triangles marked as in figure 10 sends triangles marked  $t$  to a triangle marked  $-1 - t \pmod{4km}$ . If we reduce this map modulo  $4m$ , then we see  $t \mapsto -1 - t \pmod{4m}$ . Thus, the diagram commutes for  $x = i$  and  $x' = i$ .

2.  $\rho_{2km}(j)$  acts on the marked triangles as  $t \mapsto 1 - t \pmod{4km}$ . Again, this reduces to the action of  $\rho_{2m}(j)$  modulo  $4m$ .
3. The action of  $\rho_{2km}(h)$  on the marking is

$$t \mapsto \begin{cases} t + 2km + 1 \pmod{4km} & \text{if } t \text{ is even} \\ t + 2km - 1 \pmod{4km} & \text{if } t \text{ is odd} \end{cases}$$

If  $k$  is odd then  $2km \equiv 2m \pmod{4m}$  and so if  $x = h$  we can choose  $x' = h$ . If  $k$  is even, then we need to find an  $x'$  which preserves the triangulation and sends

$$t \mapsto \begin{cases} t + 1 \pmod{4m} & \text{if } t \text{ is even} \\ t - 1 \pmod{4m} & \text{if } t \text{ is odd} \end{cases}$$

We can choose  $x' = h \circ (i \circ j)^m$ . The action of the  $(i \circ j)^m$  rotates the top  $2m$ -gon by  $\pi$  about  $A$ .

4. We will show for  $x = D$  we can take  $x' = D$ . This argument is longer, so we continue it below:

To analyze the case  $x = D$ , we introduce a useful organizing proposition:

**Proposition 14** *Let  $\psi : S_1 \rightarrow S_2$  be a branched cover between surfaces. Let  $\gamma = \{\gamma_1, \dots, \gamma_n\}$  be a collection of curves on  $S_1$  and let  $\eta$  be a curve on  $S_2$ . Let  $D_\gamma$  and  $D_\eta$  denote the action of Dehn twists in the curve families on the homology groups  $H_1(S_1)$  and  $H_1(S_2)$  respectively. Then the diagram*

$$\begin{array}{ccc} H_1(S_1) & \xrightarrow{D_\gamma} & H_1(S_1) \\ \psi \downarrow & & \psi \downarrow \\ H_1(S_2) & \xrightarrow{D_\eta} & H_1(S_2) \end{array}$$

*commutes if*

1. *for all  $\gamma_i \in \gamma$ , we have  $\psi(\llbracket \gamma_i \rrbracket) = \llbracket \eta \rrbracket$ , and*
2.  *$\llbracket \gamma \rrbracket = \llbracket \psi^{-1}(\eta) \rrbracket$ .*

**Proof:** Let  $i$  denote the algebraic intersection between two homology classes. The action of  $D_\eta \circ \psi$  is given by

$$D_\eta \circ \psi(\llbracket x \rrbracket) = \psi(\llbracket x \rrbracket) + i(\llbracket \eta \rrbracket, \psi(\llbracket x \rrbracket))\llbracket \eta \rrbracket \quad (13)$$

The action of  $D_\gamma$  on homology is

$$D_\eta(\llbracket x \rrbracket) = \llbracket x \rrbracket + \sum_{j=1}^n i(\llbracket \gamma_j \rrbracket, \llbracket x \rrbracket) \llbracket \gamma_j \rrbracket$$

When composed with  $\psi$ , by item 1 we see

$$\psi \circ D_\eta(\llbracket x \rrbracket) = \psi(\llbracket x \rrbracket) + \left( \sum_{j=1}^n i(\llbracket \gamma_j \rrbracket, \llbracket x \rrbracket) \right) \llbracket \eta \rrbracket \quad (14)$$

By item 2,

$$\sum_{j=1}^n i(\llbracket \gamma_j \rrbracket, \llbracket x \rrbracket) = i(\llbracket \gamma \rrbracket, \llbracket x \rrbracket) = i(\llbracket \psi^{-1}(\eta) \rrbracket, \llbracket x \rrbracket) = i(\llbracket \eta \rrbracket, \psi(\llbracket x \rrbracket)) \quad (15)$$

Thus, equations 14 and 15 can be combined and compared to 13 to see that  $\psi \circ D_\eta(\llbracket x \rrbracket) = D_\eta \circ \psi(\llbracket x \rrbracket)$ .  $\diamond$

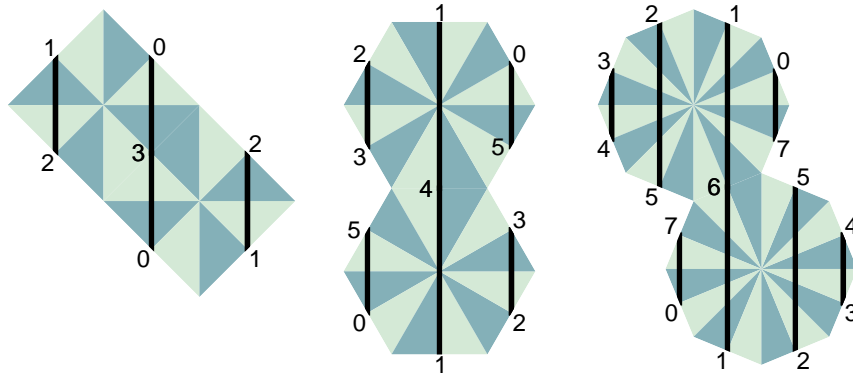


Figure 12: The Dehn twist  $D$  acts by twists in these curves. Compare to figure 6.

We will use this proposition to prove that the diagram

$$\begin{array}{ccc}
H_1(MT_{2km} \setminus \Sigma', \mathbb{Z}) & \xrightarrow{\rho_{2km}(D)} & H_1(MT_{2km} \setminus \Sigma', \mathbb{Z}) \\
\psi_k \downarrow & & \psi_k \downarrow \\
H_1(MT_{2m} \setminus \Sigma', \mathbb{Z}) & \xrightarrow{\rho_{2m}(D)} & H_1(MT_{2m} \setminus \Sigma', \mathbb{Z})
\end{array} \tag{16}$$

commutes. The curves that  $\rho_{2km}(D)$  and  $\rho_{2m}(D)$  twist in lie in the center of each of the vertical cylinders. These curves are depicted in figure 12. We need a naming scheme for the curves involved. Number the midpoints of the long edge of each triangle in the triangulation of  $MT_{2km}$  by the elements of  $\mathbb{Z}/2km\mathbb{Z}$  as in the figure. Then, we describe the curves we are interested in by a pair of integers corresponding to the two labeled midpoints that the geodesic passes through. Let  $\gamma(a, b)$  denote the geodesic loop on  $MT_{2km}$  which travels from  $a$  to  $b$  in the top  $2km$ -gon and then from  $b$  to  $a$  in the bottom  $2km$ -gon. The curves  $\rho_{2km}(D)$  twists in are in the collection

$$\gamma = \{ \gamma(0, -1), \gamma(1, -2), \dots, \gamma(km - 2, -km - 1), \gamma(km - 1, -km) \} \tag{17}$$

Similarly, we label the midpoints of the long edges of the triangulation on  $MT_{2m}$  by the elements of  $\mathbb{Z}/2m\mathbb{Z}$ . Name geodesics which pass through the midpoints on  $MT_{2m}$ ,  $\eta(a, b)$ , for elements  $a$  and  $b$ . The Dehn twist  $\rho_{2m}(D)$  acts by Dehn twists in the curve family

$$\eta = \{ \eta(0, -1), \eta(1, -2), \dots, \eta(m - 1, -m) \} \tag{18}$$

The covering map  $\psi_k$  sends midpoints marked  $t$  to midpoints marked  $t \pmod{2m}$ . Therefore,

$$\psi_k(\llbracket \gamma(a, b) \rrbracket) = \llbracket \eta(a \pmod{2m}, b \pmod{2m}) \rrbracket \tag{19}$$

We cannot apply proposition 14 directly, because  $\eta$  is a collection of curves. But we can apply it in pieces. Let  $0 \leq a < m$  and let  $\eta_a \in \eta$  denote the curve  $\eta(a, -1 - a)$  on  $MT_{2m}$ . Let  $\gamma_a \subset \gamma$  be the collection of curves on  $MT_{2m}$  given by

$$\gamma_a = \{ \gamma(a', -1 - a') \text{ such that } a' \equiv a \pmod{2m} \text{ and } 0 \leq a' < 2km \}$$

This is the collection of curves in  $\gamma$  (with modified orientations) whose homology classes are sent to  $\llbracket \eta_a \rrbracket$  by  $\psi_k$ . The curves in  $\gamma_a$  and  $\eta_a$  are shown in

figure 13 for the parameters  $m = 4$ ,  $k = 3$ ,  $a = 0$ . I claim that the action of Dehn twisting in the collection of curves  $\gamma_a$  on  $MT_{2km}$  corresponds to a Dehn twist in the curve  $\eta_a = \eta(a, -1 - a) \in \eta$  on  $MT_{2m}$  in the sense that the following diagram commutes

$$\begin{array}{ccc}
H_1(MT_{2km} \setminus \Sigma', \mathbb{Z}) & \xrightarrow{D_{\gamma_a}} & H_1(MT_{2km} \setminus \Sigma', \mathbb{Z}) \\
\psi_k \downarrow & & \psi_k \downarrow \\
H_1(MT_{2m} \setminus \Sigma', \mathbb{Z}) & \xrightarrow{D_{\eta_a}} & H_1(MT_{2m} \setminus \Sigma', \mathbb{Z})
\end{array} \tag{20}$$

To show this, we will verify the conditions of proposition 14. First note that by equation 19, we know that each curve  $\gamma(a', -1 - a') \in \gamma_a$  has the property that

$$\psi_k(\llbracket \gamma(a', -1 - a') \rrbracket) = \llbracket \eta_a \rrbracket$$

Therefore, to show this diagram commutes, it is enough to show that  $\llbracket \gamma_a \rrbracket = \llbracket \psi_k^{-1}(\eta_a) \rrbracket$ .

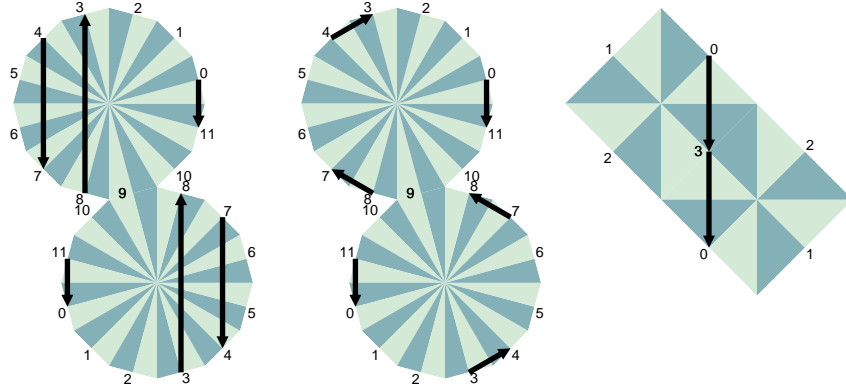


Figure 13:  $\phi_3$  is the covering  $MT_{12} \rightarrow MT_4$ . From left to right we show the curves in  $\gamma_0$ ,  $\psi_k^{-1}(\eta_0)$ , and  $\eta_0$ .

Consider the collection of preimages of the curve  $\eta_a = \eta(a, -1 - a)$  under the covering  $\psi_k$ .  $\eta_a$  enters the top  $2m$ -gon through the midpoint  $a$  and leaves through  $-1 - a$ . Therefore,  $\psi_k^{-1}(\eta_a)$  enters the top  $2km$ -gon through midpoints marked  $a' \equiv a \pmod{2m}$  and leaves the top  $2km$ -gon through midpoints marked  $-1 - a' \equiv -1 - a \pmod{2m}$ . Notice that this is the same

collection of midpoints points that the curve family  $\gamma_a$  enters and leaves through.

To show that item 2 of proposition 14 hold, we will show that  $[\gamma_a] - [\psi_k^{-1}(\eta_a)] = 0$  in  $H_1(MT_{2km} \setminus \Sigma', \mathbb{Z})$ . Consider walking along a curve in  $\gamma_a$  in the top  $2km$ -gon until you hit a midpoint. Then we can continue by walking along a curve in  $-\psi_k^{-1}(\eta_a)$  in the top  $2km$ -gon until we hit another midpoint. Then we can turn and walk along  $\gamma_a$  again staying within the top  $2km$ -gon. Eventually, our walk must close up. We can build a collection of curves in  $MT_{2km}$  in this way which is homologically equivalent to  $[\gamma_a] - [\zeta_a]$ . Each curve lies in the top or the bottom  $2km$ -gon, and is therefore contractible in  $MT_{2km} \setminus \Sigma'$ . Thus  $[\gamma_a] - [\psi_k^{-1}(\eta_a)] = 0$ . We have demonstrated that diagram 20 holds.

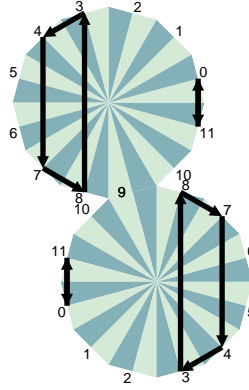


Figure 14: Continuing figure 13, we show the curves in  $\gamma_2 - \zeta_2$ .

The original curve collections  $\gamma$  and  $\eta$  of equations 17 and 18 satisfy

$$\gamma = \bigcup_{0 \leq a < m} \zeta_a \quad \text{and} \quad \eta = \bigcup_{0 \leq a < m} \eta_a \quad (21)$$

up to sign (which is irrelevant since  $D_c = D_{-c}$  for any curve  $c$ ). Therefore, the commutativity of diagram 20 implies the commutativity of diagram 16. This concludes the proof of lemma 12.  $\diamond$



## References

- [MT02] Howard Masur and Serge Tabachnikov, *Rational billiards and flat structures*, Handbook of dynamical systems, Vol. 1A, North-Holland, Amsterdam, 2002, pp. 1015–1089. MR 1928530 (2003j:37002)
- [Tab95] Serge Tabachnikov, *Billiards*, Panor. Synth. (1995), no. 1, vi+142. MR 1328336 (96c:58134)
- [Vee89] W. A. Veech, *Teichmüller curves in moduli space, Eisenstein series and an application to triangular billiards*, Invent. Math. **97** (1989), no. 3, 553–583. MR MR1005006 (91h:58083a)
- [Vee92] William A. Veech, *The billiard in a regular polygon*, Geom. Funct. Anal. **2** (1992), no. 3, 341–379. MR MR1177316 (94a:11074)